Journal of Solid Mechanics Vol. 14, No. 3 (2022) pp. 272-290
DOI: 10.22034/jsm.2019.583270.1375

Research Paper

Dynamic Stability Analysis of Bi-Directional Functionally Graded Beam with Various Shear Deformation Theories Under Harmonic Excitation and Thermal Environment

A. Ghorbanpour Arani *, Sh. Niknejad, A. Mihankhah, I. Safari

Mechanical Engineering Faculty, University of Kashan, Kashan, Iran

Received 20 March 2022; accepted 20 May 2022

ABSTRACT

In this article, dynamic stability analysis of bi-directional functionally graded materials (BDFGMs) beam rested on visco-Pasternak foundation under harmonic excitation is studied. Also, BDFGMs beam is subjected to a transversely uniformly distributed temperature rising and it is assumed that the material properties to be temperature-dependent. According to the exponential and power law distributions, thermo-mechanical properties of BDFGMs beam vary continuously in both the thickness and longitudinal directions. Based on various shear deformation theories (e.g. Euler-Bernoulli, Timoshenko, third order shear deformation and sinusoidal shear deformation theories), the stability equations of BDFGMs beam is derived by applying the Hamilton's principle. The generalized differential quadrature method (GDQM) in conjunction with the Bolotin method is utilized to solve the differential stability equations under SS, SC and CC boundary conditions. To validate the present analysis, a comparison study is carried out with the results found in the literature and a good agreement is observed compared to the reported results. Finally, numerical results are presented to study the influences of the gradient index, length-to-thickness ratio, temperature rise and foundation parameters on the dynamic stability region of BDFGMs beam. The results of presented paper can be used to the optimal design and assessment of the structural failure.

Keywords : Dynamic stability; Bi-directional functionally graded materials; Various shear deformation theories; Thermal environment; Harmonic excitation.

1 INTRODUCTION

FUNCTIONALLY graded materials (FGMs) were first proposed in 1984 by a group of Japanese scientists in Sendai and very soon have become very popular in research and engineering applications. These materials are

*Corresponding author. Tel.: +98 3155912450; Fax: +98 3155912424.
E-mail address: aghorban@kashanu.ac.ir (A.Ghorbanpour Arani)

made of two (or more) different materials which their properties vary continuously in desired directions. Due to the high resistance heat capacity of ceramic and good mechanical properties of metal, FGMs structures composed of these two materials are widely used in high temperature applications, such as the spacecraft, nuclear reactors or structures for the chemical industry and defence. Also, these structures are often under the different types of dynamic loads, among which the periodically time-varying force may cause dynamic instability through parametric resonance. Thus, a comprehensive research about the dynamic stability characteristics of FGMs structures in thermal environments is a matter of considerable importance for the optimal design and assessment of the structural failure.

The dynamic response of ordinary FGMs beams under dynamic loads has been widely studied by many researchers. Li [1] presented a unified approach for analyzing static and dynamic behaviors of FG Timoshenko and Euler–Bernoulli beams. He assumed that all material properties are arbitrary functions along the beam thickness. Piovan and Machado [2] considered thermo-elastic dynamic stability of FG thin-walled beams subjected to axial external dynamic loading. They used Galerkin's and Bolotin's methods with the scope to discretize the equations of motion and to obtain the regions of dynamic stability, respectively. Mohanty et al. [3] investigated the dynamic stability of ordinary FG beam and FG sandwich beam on Winkler's elastic foundation using finite element method (FEM). They considered that the material properties vary continuously based on exponential and power law. Yan et al. [4] studied the dynamic response of FG beams with an open edge crack resting on an elastic foundation subjected to a transverse load moving at a constant speed. By applying an exponential variation for material properties through the thickness direction, they derived the governing equations of motion by using Hamilton's principle. Based on the modified couple stress theory (MCST), dynamic stability of micro-beams made of FGMs were investigated by Ke and Wang [5]. They estimated the material properties of FGM microbeams along the thickness direction according to the Mori–Tanaka homogenization technique and obtained the higher-order governing equations and boundary conditions using the Hamilton's principle. Şimşek et al. [6] presented linear dynamic analysis of an axially FG beam with simply-supported edges under a moving harmonic load using Euler–Bernoulli beam theory. They employed Newmark method to find the dynamic responses of FG beam and discussed about the effects of material distribution, velocity of the moving load and excitation frequency on dynamic behavior of these system. Salamat-talab et al. [7] developed MCST to analyze the static and dynamic stability of third-order shear deformation FG micro-beam. While the Poisson's ratio is constant, they assumed that mechanical properties of the FG micro beam follow a power law form through thickness. Yan et al. [8] investigated the nonlinear flexural dynamic behavior of a clamped FGMs beam with an open edge crack under an axial parametric excitation which is a combination of a static compressive force and a harmonic excitation force. They derived the nonlinear partial differential equations based on Timoshenko shear deformable beam theory, von Karman type geometric nonlinearity, and rotational spring model. Dynamic analysis of FG nanocomposite beams reinforced by randomly oriented carbon nanotube under the action of moving load were studied by Yas and Heshmati [9]. They utilized the Eshelby–Mori–Tanaka approach based on an equivalent fiber to estimate the material properties of the beam. Zamanzadeh et al. [10] presented a model for static and dynamic stability of a capacitive FGM micro-beam based on MCST. They applied the nonlinear electrostatic pressure and thermal changes regarding convection and radiation on beam and by changing the ceramic constituent percent of the bottom surface, studied five different types of FGM micro-beams. Nguyen et al. [11] analyzed the dynamic response of non-uniform FG beams under a variable speed moving point load via FEM. They considered the influences of shear deformation, cross-sectional variation and the shift in the neutral axis position and formulated a beam element by using exact polynomials derived from solutions of the governing differential equations of a homogeneous Timoshenko beam element. Dynamic response of Timoshenko FG beams with classical and non-classical boundary conditions were investigated by Wattanasakulpong and Mao [12] using Chebyshev collocation method. They defined material composition across the beam thickness according to different mathematical models such as the power law, exponential and Mori–Tanaka models. Nonlinear dynamic buckling and imperfection sensitivity of the FGM Timoshenko beam subjected to sudden uniform temperature rise were presented by Ghiasian et al. [13]. They employed the Budiansky–Roth criterion to detect the unbounded motion type of dynamic buckling and observed that for beams with stable post-buckling equilibrium path, no dynamic buckling occurs according to the Budiansky–Roth criterion. Gan et al. [14] developed a FEM for dynamic analysis of non-uniform Timoshenko beams made of axially FGMs subjected to the multiple moving point loads. They assumed that the material properties change in the longitudinal direction according to a power law equation. Wang and Wu [15] studied thermal effect on the dynamic response of axially FG beam subjected to a moving harmonic load within the frameworks of classical beam theory and Timoshenko beam theory. They utilized the Lagrange method to obtain the thermal buckling equations and then, with the critical buckling temperature as a parameter, evaluated the dynamic response of system under thermal environments via Newmark-β method. Based on the first-order shear deformation theory (FSDT), Malekzadeh and Monajjemzadeh [16] investigated the dynamic response of FG beams in thermal environment under a moving load. They considered FEM to develop a solution approach for FG beams with general

loading and boundary conditions. Wu et al. [17] analyzed the dynamic instability of FG multilayer nanocomposite beams reinforced with a low content of graphene nanoplatelets (GPLs). They applied a periodic axial force with a temperature change on beam and indicated that distributing more GPLs near the top and bottom surfaces can effectively increase the natural frequency and reduce the size of the unstable region. By considering surface effects according to Gurtin-Murdoch continuum theory, Saffari et al. [18] presented the dynamic stability of FG nano-beam resting on Pasternak elastic medium based on nonlocal Timoshenko theory. Recently, Nguyen et al. [19] developed a higher-order finite beam element for dynamic analysis of FG Timoshenko beams in thermal environment using hierarchical functions. They considered the effect of environmental temperature in the element derivation by assuming that the material properties are temperature-dependent.

However, dynamic stability analysis of bi-directional functionally graded materials (BDFGMs) beam rested on visco-Pasternak substrate is a novel topic that it hasn't been found in literature. Motivated by these considerations, our aim is to study of thermo-mechanical dynamic stability analysis of BDFGMs beam which is placed in uniform temperature and harmonic excitation. It is assumed that the temperature-dependent material properties vary continuously in both the thickness and longitudinal directions according to the exponential and power law distributions. Four shear deformation beam theories include Euler-Bernoulli beam theory (EBT), Timoshenko beam theory (TBT), third order shear deformation beam theory (TSDT) and sinusoidal shear deformation beam theory (SSDT) are used to develop the governing stability equations of BDFGMs beam and solved by the generalized differential quadrature method (GDQM) in conjunction with the Bolotin method.

2 BI-DIRECTIONAL FUNCTIONALLY GRADED MATERIAL (BDFGM)

In this article, it is suggested two types of distributions include the exponential and power law models for predicting the material properties of BDFGM beam such as Young's modulus E, shear modulus G, thermal expansion α and mass density ρ (except for Poisson's ratio υ) vary in both axial and transverse directions. On the other hand, four different materials include two ceramics (referred to as P_{c1} and P_{c2}) and two metals (referred to as P_{m1} and P_{m2}) are selected as the constituent materials of BDFGMs beam which are shown in Fig. 1. Also, all material properties are considered to be temperature-dependent. Thus, a typical material property P must be a function of environment temperature $T(K)$ which can be given by [20]:

$$P_{c1,c2,m1,m2} = P_0\left(P_{-1}T^{-1} + 1 + P_1T + P_2T^2 + P_3T^3\right), \tag{1}$$

In which, P_0, P_{-1}, P_1, P_2 and P_3 are the coefficients of constituent materials depend on the temperature.

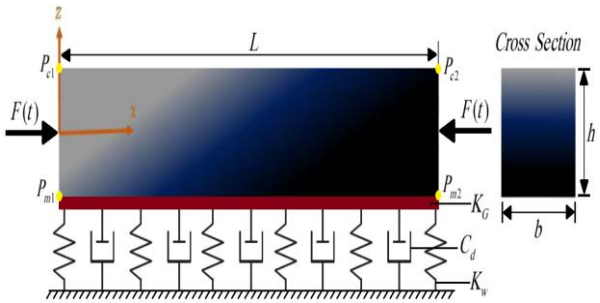

Fig.1
BDFGMs beam rested on visco-Pasternak foundation under a harmonic axial force and thermal environment.

2.1 Power law model

Based on the rule of mixture, the effective material properties of BDFGM beam can be expressed as [21]:

$$P\left(x,z,T\right) = V_{c1}P_{c1} + V_{c2}P_{c2} + V_{m1}P_{m1} + V_{m2}P_{m2}, \tag{2}$$

where V is the volume fraction of materials which change along the x and z axes of beam as follows:

$$V_{m1}=\left[1-\left(\frac{z}{h}+\frac{1}{2}\right)^{n_z}\right]\left[1-\left(\frac{x}{L}\right)^{n_x}\right], \tag{3a}$$

$$V_{m2}=\left[1-\left(\frac{z}{h}+\frac{1}{2}\right)^{n_z}\right]\left(\frac{x}{L}\right)^{n_x}, \tag{3b}$$

$$V_{c1}=\left(\frac{z}{h}+\frac{1}{2}\right)^{n_z}\left[1-\left(\frac{x}{L}\right)^{n_x}\right], \tag{3c}$$

$$V_{c2}=\left(\frac{z}{h}+\frac{1}{2}\right)^{n_z}\left(\frac{x}{L}\right)^{n_x}, \tag{3d}$$

In Eq. (3), n_z and n_x represent the grading indexes and indicate the variation of the constituent materials in the thickness and longitudinal directions, respectively. By substituting Eq. (3) into Eq. (2), the following relation can be obtained as:

$$P=\left[P_{m1}+\left(P_{c1}-P_{m1}\right)\left(\frac{z}{h}+\frac{1}{2}\right)^{n_z}\right]\left[1-\left(\frac{x}{L}\right)^{n_x}\right]+\left[P_{m2}+\left(P_{c2}-P_{m2}\right)\left(\frac{z}{h}+\frac{1}{2}\right)^{n_z}\right]\left(\frac{x}{L}\right)^{n_x}, \tag{4}$$

2.2 Exponential law model

Based on the exponential law model, the effective material properties of BDFGMs beam can be obtained from [22]:

$$P\left(x,z,T\right)=\frac{P_{m1}}{1-e}\left[\exp\left(\frac{x}{L}\right)^{n_x}-e\right]\exp\left[\ln\left(\frac{P_{c1}}{P_{m1}}\right)\left(\frac{1}{2}+\frac{z}{h}\right)^{n_z}\right]+\frac{P_{m2}}{1-e}\left[1-\exp\left(\frac{x}{L}\right)^{n_x}\right]\exp\left[\ln\left(\frac{P_{c2}}{P_{m2}}\right)\left(\frac{1}{2}+\frac{z}{h}\right)^{n_z}\right], \tag{5}$$

Hence, in both exponential and power law models, the beam becomes homogeneous by inserting $n_x=n_y=0$.

3 GEOMETRY AND GOVERNING EQUATIONS

A BDFGMs beam with length *L*, width *b* and thickness *h* subjected to harmonic axial force *F*(*t*) and thermal environment is shown in Fig. 1 where the Cartesian coordinate system (*x*, *z*) is specified on these figure. Also, beam is rested on visco-Pasternak foundation includes springs (K_w), dampers (C_d) and shear layer (K_G).

In this article, four shear deformation beam theories include EBT, TBT, TSDT and SSDT are selected as the displacement field of BDFGMs beam. In general form, the displacement field can be written as:

$$u_x\left(x,z,t\right)=u\left(x,t\right)+f\left(z\right)\frac{\partial w\left(x,t\right)}{\partial x}+g\left(z\right)\varphi\left(x,t\right), \tag{6a}$$

$$u_z\left(x,z,t\right)=w\left(x,t\right), \tag{6b}$$

where, *u* and *w* are the displacement components in the mid-plane along the coordinates *x* and *z*, respectively. Also, φ is the rotation of the cross section about the *y* axis. In accordance with arbitrary shear deformation beam theories, functions $f\left(z\right)$ and $g\left(z\right)$ can be defined as:

$$\text{EBT: } f(z) = -z, \text{ and } g(z) = 0, \tag{7a}$$

$$\text{TBT: } f(z) = 0, \text{ and } g(z) = z, \tag{7b}$$

$$\text{TSDT: } f(z) = -\frac{4z^3}{3h^2}, \text{ and } g(z) = z - \frac{4z^3}{3h^2}, \tag{7c}$$

$$\text{SSDT: } f(z) = -z, \text{ and } g(z) = \frac{h}{\pi}\sin\left(\frac{\pi}{h}z\right). \tag{7d}$$

The strain-displacement relations can be expressed as:

$$\begin{aligned} \varepsilon_{xx} &= \frac{\partial u_x}{\partial x} = \frac{\partial u}{\partial x} + f\frac{\partial^2 w}{\partial x^2} + g\frac{\partial \varphi}{\partial x}, \\ \gamma_{xz} &= \frac{\partial u_x}{\partial z} + \frac{\partial u_z}{\partial x} = \left[1 + \frac{df}{dz}\right]\frac{\partial w}{\partial x} + \frac{dg}{dz}\varphi, \end{aligned} \tag{8}$$

In which, ε_{xx} and γ_{xz} indicate normal and shear strains, respectively. Based on the Hook's law, the constitutive equation can be written as follows:

$$\begin{aligned} \sigma_{xx} &= E(x,z,T)\left[\varepsilon_{xx} - \alpha(x,z,T)T\right], \\ \tau_{xz} &= kG(x,z,T)\gamma_{xz}, \end{aligned} \tag{9}$$

where σ_{xx} is normal stress and τ_{xz} is shear stresse. Also, the shear correction factor *k* can be obtained from:

$$k_{EBT} = 0, k_{TBT} = \frac{5+5\upsilon}{6+5\upsilon}, k_{TSDBT} = k_{SSDBT} = 1. \tag{10}$$

The governing differential equations of BDFGMs beam subjected to the harmonic axial force and thermal environment can be derived from Hamilton's principle [23]:

$$\int_0^t \delta\left(T - U + W_{ext}\right)dt = 0, \tag{11}$$

In which, *T*, *U* and W_{ext} refer to the kinetic energy, the strain energy and the work done by external loads, respectively. The kinetic energy for a beam can be determined with the following equations:

$$T = \frac{1}{2}\int_{\forall} \rho(x,z,T)\left[\left(\frac{\partial u_x}{\partial t}\right)^2 + \left(\frac{\partial u_z}{\partial t}\right)^2\right]d\forall, \tag{12}$$

where $\forall$ is the volume of beam. Using Eq. (6), variations of kinetic energy can be defined as:

$$T = \frac{1}{2}\int_0^L \left[\begin{aligned} &I_1\left(\frac{\partial u}{\partial t}\right)^2 + I_1\left(\frac{\partial w}{\partial t}\right)^2 + 2I_2\frac{\partial u}{\partial t}\frac{\partial^2 w}{\partial t\,\partial x} + 2I_3\frac{\partial u}{\partial t}\frac{\partial \varphi}{\partial t} \\ &+I_4\left(\frac{\partial^2 w}{\partial t\,\partial x}\right)^2 + 2I_5\frac{\partial^2 w}{\partial t\,\partial x}\frac{\partial \varphi}{\partial t} + I_6\left(\frac{\partial \varphi}{\partial t}\right)^2 \end{aligned}\right]dx, \tag{13}$$

where

$$I_{1,2,3,4,5,6} = \int_{-\frac{h}{2}}^{\frac{h}{2}} \int_{-\frac{b}{2}}^{\frac{b}{2}} \rho(x,z,T)\left[1, f, g, f^2, fg, g^2\right] dydz . \tag{14}$$

Variations of strain energy can be expressed as follows:

$$\delta U = \int_{\forall} \left(\sigma_{ij}\, \delta\varepsilon_{ij}\right) d\forall = \int_{\forall} \left(\sigma_{xx}\, \delta\varepsilon_{xx} + \tau_{xz}\, \delta\gamma_{xz}\right) d\forall, \tag{15}$$

Substituting Eqs. (6) and (9) into Eq. (15) yields:

$$\delta U = \int_0^L \left(N_x \frac{\partial \delta u}{\partial x} + M_x \frac{\partial^2 \delta w}{\partial x^2} + P_x \frac{\partial \delta \varphi}{\partial x} + Q_x \frac{\partial \delta w}{\partial x} + R_x \delta\varphi \right) dx \tag{16}$$

where

$$N_x, M_x, P_x = \int_{-\frac{h}{2}}^{\frac{h}{2}} \int_{-\frac{b}{2}}^{\frac{b}{2}} \sigma_x \left(1, f, g\right) dydz , \quad Q_x, R_x = \int_{-\frac{h}{2}}^{\frac{h}{2}} \int_{-\frac{b}{2}}^{\frac{b}{2}} \tau_{xz} \left[\left(1 + \frac{df}{dz}\right), \frac{dg}{dz}\right] dydz , \tag{17}$$

The external work variation done by the harmonic axial force [24], thermal loading [25] and visco-Pasternak medium force [26] can be given by:

$$\delta W_{ext} = \int_0^L \left[F_f\, \delta w - \left(F(t) - N^T\right) \frac{\partial w}{\partial x} \frac{\partial \delta w}{\partial x} \right] dx , \tag{18}$$

where

$$\begin{aligned} &F(t) = N_{static} + N_{dynamic} \cos\left(\Omega t\right) = \alpha N_{cr} + \beta N_{cr} \cos\left(\Omega t\right), \\ &N^T(x) = \int_{-\frac{b}{2}}^{\frac{b}{2}} \int_{-\frac{h}{2}}^{\frac{h}{2}} E(x,z)\, \alpha(x,z)\, \Delta T dz\, dy , \\ &F_f = -K_w w + K_G \frac{\partial^2 w}{\partial x^2} - C_d \frac{\partial w}{\partial t}, \end{aligned} \tag{19}$$

In which, α and β are static and dynamic load factors, respectively. Also, Ω is the frequency of excitation or pulsation frequency. By introducing Eqs. (13), (16) and (18) into Eq. (11) and putting the coefficients of δu , δw and $\delta\varphi$ to zero, the differential equations of motion of present system can be given by:

$$\frac{\partial N_x}{\partial x} - I_1 \frac{\partial^2 u}{\partial t^2} - I_2 \frac{\partial^3 w}{\partial t^2 \partial x} - I_3 \frac{\partial^2 \varphi}{\partial t^2} = 0, \tag{20a}$$

$$\frac{\partial^2 M_x}{\partial x^2} - \frac{\partial Q_x}{\partial x} - F_f - F(t) \frac{\partial^2 w}{\partial x^2} + \frac{\partial}{\partial x}\left(N^T \frac{\partial w}{\partial x} \right) + I_1 \frac{\partial^2 w}{\partial t^2} - I_4 \frac{\partial^4 w}{\partial t^2 \partial x^2} - I_2 \frac{\partial^3 u}{\partial t^2 \partial x} - I_5 \frac{\partial^3 \varphi}{\partial t^2 \partial x} = 0, \tag{20b}$$

$$\frac{\partial P_x}{\partial x} - R_x - I_6 \frac{\partial^2 \varphi}{\partial t^2} - I_3 \frac{\partial^2 u}{\partial t^2} - I_5 \frac{\partial^3 w}{\partial t^2 \partial x} = 0, \tag{20c}$$

The expression of boundary conditions for clamped and simply supported edges (x=0, L) of the beam can be defined as:

a) Clamped

$$u = w = \varphi = 0,\ \frac{\partial w}{\partial x} = 0, \tag{21a}$$

b) Simply supported

$$u = w = 0,\ M_x = P_x = 0, \tag{21b}$$

The relations between stress resultants and displacement components can be determined by inserting Eq. (6) into Eq. (17):

$$N_x = A_1 \frac{\partial u}{\partial x} + A_2 \frac{\partial^2 w}{\partial x^2} + A_3 \frac{\partial \varphi}{\partial x}, \tag{22a}$$

$$M_x = A_2 \frac{\partial u}{\partial x} + A_4 \frac{\partial^2 w}{\partial x^2} + A_5 \frac{\partial \varphi}{\partial x}, \tag{22b}$$

$$P_x = A_3 \frac{\partial u}{\partial x} + A_5 \frac{\partial^2 w}{\partial x^2} + A_6 \frac{\partial \varphi}{\partial x}, \tag{22c}$$

$$Q_x = A_7 \frac{\partial w}{\partial x} + A_8 \varphi, \tag{22d}$$

$$R_x = A_8 \frac{\partial w}{\partial x} + A_9 \varphi, \tag{22e}$$

where

$$\begin{aligned} A_{1,2,3,4,5,6} &= \int_{-\frac{h}{2}}^{\frac{h}{2}} \int_{-\frac{b}{2}}^{\frac{b}{2}} E(x,z,T)\left[1, f, g, f^2, fg, g^2\right] dydz, \\ A_{7,8,9} &= \int_{-\frac{h}{2}}^{\frac{h}{2}} \int_{-\frac{b}{2}}^{\frac{b}{2}} G(x,z,T)\left[\left(1+\frac{df}{dz}\right)^2, \frac{dg}{dz}\left(1+\frac{df}{dz}\right), \left(\frac{dg}{dz}\right)^2\right] dydz, \end{aligned} \tag{23}$$

Substituting Eq. (22) into Eqs. (20) and (21), the differential equations of motion and boundary conditions of BDFGMs beam in terms of the displacements can be derived as follows:

$$A_1 \frac{\partial^2 u}{\partial x^2} + \frac{dA_1}{dx}\frac{\partial u}{\partial x} + A_2 \frac{\partial^3 w}{\partial x^3} + \frac{dA_2}{dx}\frac{\partial^2 w}{\partial x^2} + A_3 \frac{\partial^2 \varphi}{\partial x^2} + \frac{dA_3}{dx}\frac{\partial \varphi}{\partial x} - I_1 \frac{\partial^2 u}{\partial t^2} - I_2 \frac{\partial^3 w}{\partial t^2 \partial x} - I_3 \frac{\partial^2 \varphi}{\partial t^2} = 0, \tag{24a}$$

$$\begin{aligned} &+A_2 \frac{\partial^3 u}{\partial x^3} + 2\frac{dA_2}{dx}\frac{\partial^2 u}{\partial x^2} + \frac{d^2 A_2}{dx^2}\frac{\partial u}{\partial x} + A_4 \frac{\partial^4 w}{\partial x^4} + 2\frac{dA_4}{dx}\frac{\partial^3 w}{\partial x^3} + K_w w + A_5 \frac{\partial^3 \varphi}{\partial x^3} \\ &+\left(\frac{d^2 A_4}{dx^2} - A_7 - K_G + N^T\right)\frac{\partial^2 w}{\partial x^2} - F(t)\frac{\partial^2 w}{\partial x^2} - \left(\frac{dA_7}{dx} - \frac{\partial N^T}{\partial x}\right)\frac{\partial w}{\partial x} + 2\frac{dA_5}{dx}\frac{\partial^2 \varphi}{\partial x^2} \\ &+\left(\frac{d^2 A_5}{dx^2} - A_8\right)\frac{\partial \varphi}{\partial x} - \frac{dA_8}{dx}\varphi + C_d \frac{\partial w}{\partial t} - I_2 \frac{\partial^3 u}{\partial t^2 \partial x} - I_4 \frac{\partial^4 w}{\partial t^2 \partial x^2} + I_1 \frac{\partial^2 w}{\partial t^2} - I_5 \frac{\partial^3 \varphi}{\partial t^2 \partial x} = 0, \end{aligned} \tag{24b}$$

$$-I_3\frac{\partial^2 u}{\partial t^2}-I_5\frac{\partial^3 w}{\partial t^2\partial x}-I_6\frac{\partial^2 \varphi}{\partial t^2}+A_3\frac{\partial^2 u}{\partial x^2}+\frac{dA_3}{dx}\frac{\partial u}{\partial x}+A_5\frac{\partial^3 w}{\partial x^3}+\frac{dA_5}{dx}\frac{\partial^2 w}{\partial x^2}-A_8\frac{\partial w}{\partial x}+A_6\frac{\partial^2 \varphi}{\partial x^2}+\frac{dA_6}{dx}\frac{\partial \varphi}{\partial x}-A_9\varphi=0, \tag{24c}$$

a) Clamped

$$u=w=\varphi=0,\ \frac{\partial w}{\partial x}=0, \tag{25a}$$

b) Simply supported

$$\begin{aligned} &u=w=0,\\ &A_3\frac{\partial u}{\partial x}+A_5\frac{\partial^2 w}{\partial x^2}+A_6\frac{\partial \varphi}{\partial x}=0,\\ &A_2\frac{\partial u}{\partial x}+A_4\frac{\partial^2 w}{\partial x^2}+A_5\frac{\partial \varphi}{\partial x}=0. \end{aligned} \tag{25b}$$

4 SOLUTION PROCEDURE

4.1 Generalized differential quadrature method (GDQM)

According to the GDQM, the approximation value of *rth* derivative at the *ith* discrete points for a one dimensional continuous function *f(x)* can be obtained by [27]:

$$\left.\frac{\partial^r f(x)}{\partial x^r}\right|_{x=x_i}=\sum_{j=1}^{N}A_{ij}^{(r)}f(x_j), \tag{26}$$

In which, $A_{ij}^{(r)}$ are weighting coefficients, *f(x)* can be taken as the displacement functions (i.e., *u, w* and φ) and $x_i=1,2,...,N$ are the discrete points and mostly introduced in non-uniform pattern based on the Chebyshev–Gauss–Lobatto pattern:

$$x_i=\frac{1}{2}\left[1-\cos\left(\pi\frac{i-1}{N-1}\right)\right]\quad \text{for}\quad i=1,2,...,N \tag{27}$$

Using the Lagrange interpolation functions, the weighting function associate to first order of *f(x)* can be formulated as:

$$\begin{cases} A_{ij}^{(1)}=\displaystyle\prod_{k=1,k\neq i,j}^{N}(x_i-x_k)\Big/\prod_{k=1,k\neq j}^{N}(x_j-x_k) & (i\neq j)\\ A_{ij}^{(1)}=\displaystyle\prod_{k=1,k\neq i}^{N}\frac{1}{(x_i-x_k)} & (i=j) \end{cases} \quad \text{for } i,j=1,2,...,N \tag{28}$$

and for higher-order derivatives

$$\begin{aligned} &A_{ij}^{(2)}=\sum_{k=1}^{N}A_{ik}^{(1)}A_{kj}^{(1)},\\ &A_{ij}^{(3)}=\sum_{k=1}^{N}A_{ik}^{(1)}A_{kj}^{(2)}\qquad \text{for } i,j=1,2,...,N\\ &...\\ &A_{ij}^{(r+1)}=\sum_{k=1}^{N}A_{ik}^{(1)}A_{kj}^{(r)} \end{aligned} \tag{29}$$

A set of discretized relations can be obtained for stability and boundary equations in the matrix form by substituting Eq. (26) into stability Eqs. (24) and boundary condition (25) as follows:

$$[M]\{\ddot{X}\}+[C]\{\dot{X}\}+\left([K]+P(t)[K_P]\right)\{X\}=\{0\}, \tag{30}$$

where M, C, K and K_P indicate the mass, damping, stiffness and geometrical stiffness matrices, respectively, and, X represent the displacement vector ($X=u,\varphi,w$).

4.2 Bolotin method

The dynamic instability region of present system can be achieved by Bolotin method. According to this method, the displacement vector (X) can be written in the Fourier series with the period $2T$ as follows:

$$X=\sum_{k=1,3,5,\ldots}^{\infty}\left(a_k\sin\frac{k\Omega t}{2}+b_k\cos\frac{k\Omega t}{2}\right), \tag{31}$$

In which, a_k and b_k are unknown constants. Substitute Eq. (31) into Eq. (30) and set the coefficients of each sine and cosine as well as the sum of the constant terms to zero, the final relation can be obtained as following form:

$$\left|[K]-\alpha P_{cr}[K_P]\pm P_{cr}\frac{\beta}{2}[K_P]\mp\frac{\Omega}{2}[C]-\frac{\Omega^2}{4}[M]\right|=0. \tag{32}$$

This method presented by Bolotin [28] in 1964 shows that the first instability region is wider than other regions and the structural damping becomes neutralized in higher regions. Therefore, the most important region is usually the first instability region for researchers where can be obtained by plotting the variation of Ω versus β after solving Eq. (32).

5 RESULTS AND DISCUSSION

Numerical investigations are carried out in this section to study the effects of the material distributions, length-to-thickness ratio, different boundary conditions, temperature rise and foundation coefficients on the dynamic stability region of BDFGMs beam. Silicon (Si_3N_4), zirconia (ZrO_2), stainless steel (SUS304) and titanium (Ti-6Al-4V) with temperature-dependent material properties given in Table 1 [29] are selected as ceramic1, ceramic2, metal 1 and metal 2, respectively.

Table 1
Coefficients of temperature-dependent material properties [29].

Material		Si_3N_4	ZrO_2	SUS304	Ti-6Al-4V
$E(GPa)$	P_{-1}	0	0	0	0
	P_0	348.43	132.20	201.04	122.70
	P_1	-3.070×10^{-4}	-3.805×10^{-4}	3.079×10^{-4}	-4.605×10^{-4}
	P_2	2.160×10^{-7}	-6.127×10^{-8}	-6.534×10^{-7}	0
	P_3	-8.946×10^{-11}	0	0	0
υ	P_{-1}	0	0	0	0
	P_0	0.2400	0.3330	0.3262	0.2888
	P_1	0	0	-2.002×10^{-4}	1.108×10^{-4}
	P_2	0	0	3.797×10^{-7}	0
	P_3	0	0	0	0

$\rho(\frac{Kg}{m^3})$	P_{-1}	0	0	0	0
	P_0	2370	3657	8166	4420
	P_1	0	0	0	0
	P_2	0	0	0	0
	P_3	0	0	0	0
$\alpha(\frac{1}{K})$	P_{-1}	0	0	0	0
	P_0	5.8723×10^{-6}	13.300×10^{-6}	12.330×10^{-6}	7.4300×10^{-6}
	P_1	9.095×10^{-6}	-1.421×10^{-3}	8.086×10^{-6}	7.483×10^{-4}
	P_2	0	9.546×10^{-7}	0	-3.621×10^{-7}
	P_3	0	0	0	0

Furthermore, in order to obtain the numerical results, CC boundary condition is considered for BDFGMs beam except for the cases to be mentioned and other parameters are as follows:

$$L=2m,\ h/L=0.04,\ n_x=n_z=2,\ \upsilon=0.3,\ \alpha=0.2,\ K_w=10^4\,N/m^3,\ K_G=10^3\,N/m,$$
$$C_d=50\,Ns/m^3,\ T_0=300K,\ \Delta T=100K$$

Before presenting the results, the reliability of the presented solution procedure should be investigated. Table 2 demonstrates the dimensionless frequency of simply supported BDFGMs beam obtained from present work and Refs. [30, 31] without thermal environment. As it can be seen, the present results are in excellent agreement and very small difference between three papers is due to employ various solution methods.

Table 2

Comparison of dimensionless frequency ($\bar{\omega}=\omega\frac{L^2}{h}\sqrt{\frac{\rho_{Al}}{E_{Al}}}$) of simply supported BDFGMs beam without temperature rise.

n_z	Source	n_x							
		0	1/3	1/2	5/6	1	4/3	3/2	2
0	Present	3.3032	3.7383	3.9127	4.1986	4.3171	4.5167	4.6012	4.8079
	Ref. [30]	3.3018	3.7428	3.9146	4.1966	4.3137	4.5116	4.5954	4.8003
	Ref. [31]	3.3018	3.7429	3.9148	4.1968	4.3139	4.5118	4.5956	4.8005
1/3	Present	3.2189	3.5518	3.6791	3.8759	3.9534	4.0792	4.1307	4.2526
	Ref. [30]	3.1543	3.5050	3.6305	3.8251	3.9022	4.0276	4.0791	4.2008
	Ref. [31]	3.1542	3.5050	3.6305	3.8252	3.9022	4.0277	4.0792	4.2009
1/2	Present	3.1997	3.4978	3.6099	3.7797	3.8455	3.9511	3.9939	4.0943
	Ref. [30]	3.1069	3.4258	3.5397	3.7087	3.7745	3.8805	3.9235	4.0244
	Ref. [31]	3.1068	3.4258	3.5397	3.7087	3.7745	3.8805	3.9236	4.0245
5/6	Present	3.1570	3.4080	3.4984	3.6308	3.6810	3.7601	3.7918	3.8655
	Ref. [30]	3.0505	3.3296	3.4206	3.5547	3.6058	3.6868	3.7193	3.7946
	Ref. [31]	3.0504	3.3296	3.4206	3.5548	3.6059	3.6869	3.7194	3.7947
1	Present	3.1366	3.3720	3.4542	3.5730	3.6179	3.6881	3.7161	3.7811
	Ref. [30]	3.0359	3.2983	3.3818	3.5034	3.5493	3.6217	3.6507	3.7175
	Ref. [31]	3.0359	3.2984	3.3819	3.5035	3.5495	3.6219	3.6508	3.7177

Fig. 2 illustrates the dynamic stability regions of BDFGMs beam for various boundary conditions based on four shear deformation beam theories (EBT, TBT, TSDT and SSDT). According to this figure, the dynamic instability region and the pulsation frequency for CC boundary condition is higher than SC and SS boundary conditions. Also, the pulsation frequency obtained by EBT is higher than that for other shear deformation beam theories and the results obtained by TBT, TSDT and SSDT are very close to each other. Moreover, considering power law model in order to determine the material properties of BDFGMs beam causes to obtain the lower pulsation frequency in comparison with exponential law model.

Fig. 3 indicates the dynamic stability regions of BDFGMs beam for different temperatures rise. It can be observed that by increasing temperature, the dynamic instability region shift to the lower pulsation frequency and decreases. It is due to increase the flexibility of BDFGMs beam under rising temperature.

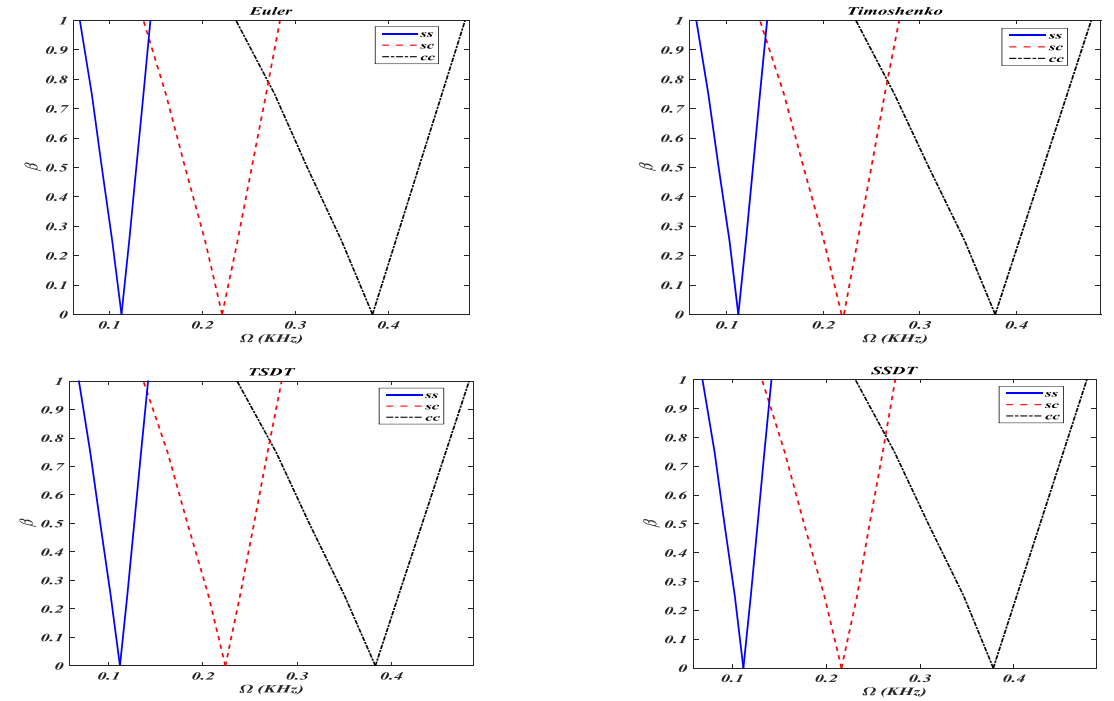

(a)

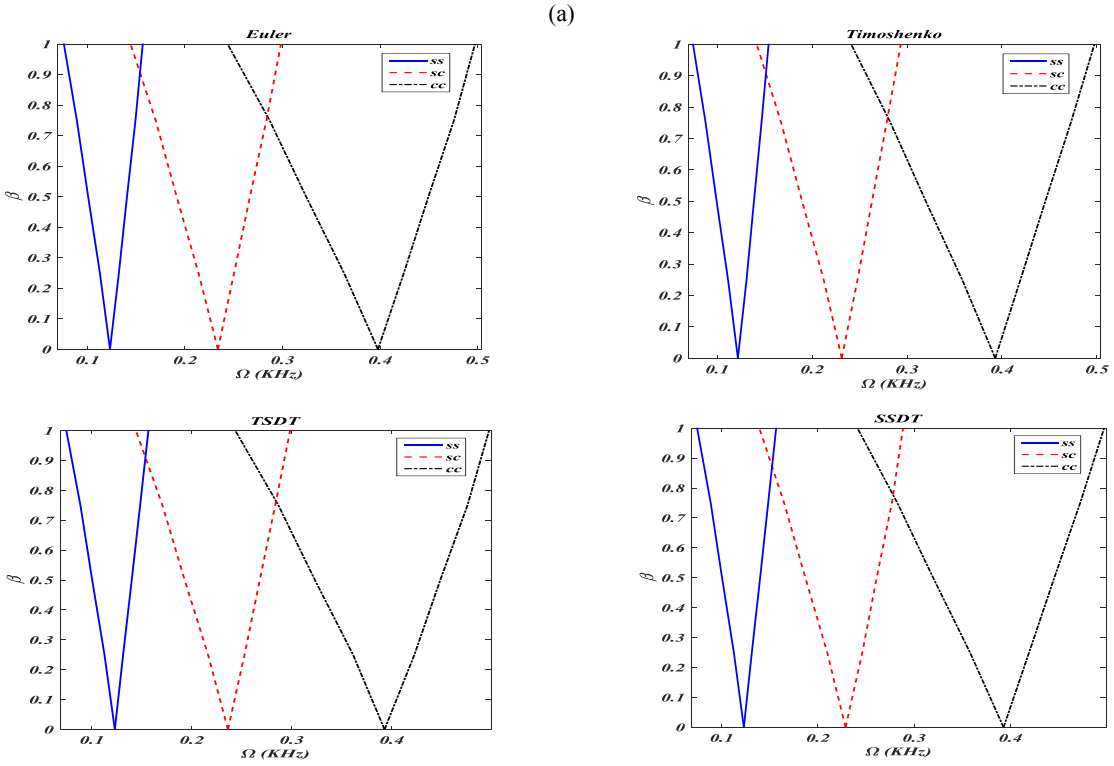

(b)

Fig.2
The dynamic stability regions of BDFGMs beam for various boundary conditions; a) power law model, b) exponential law model.

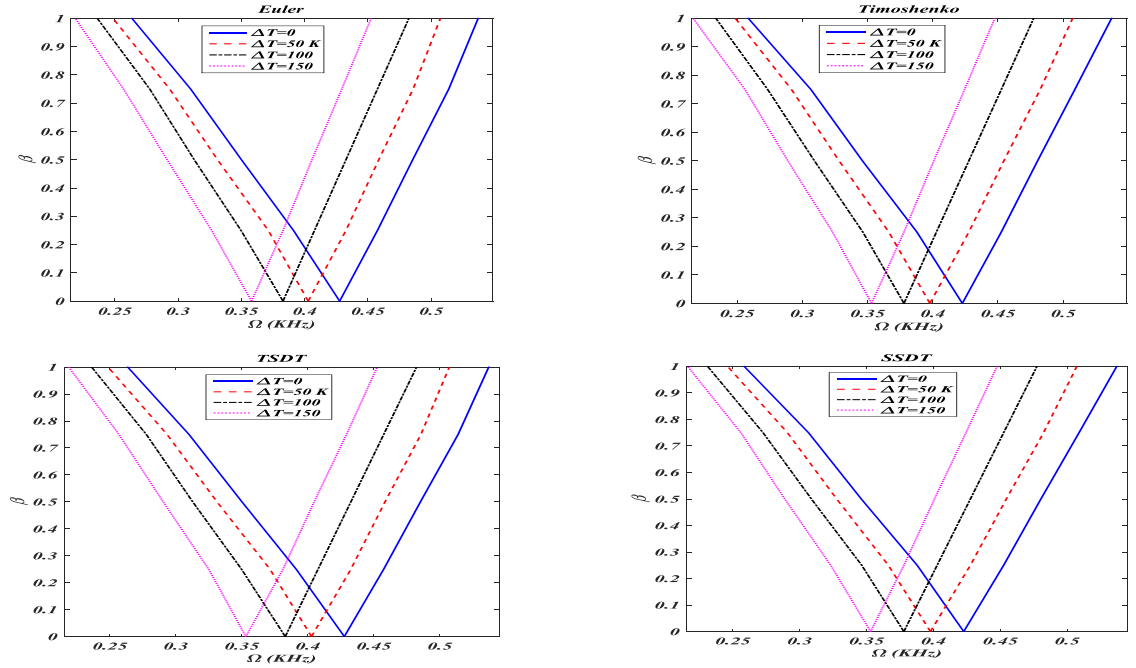

(a)

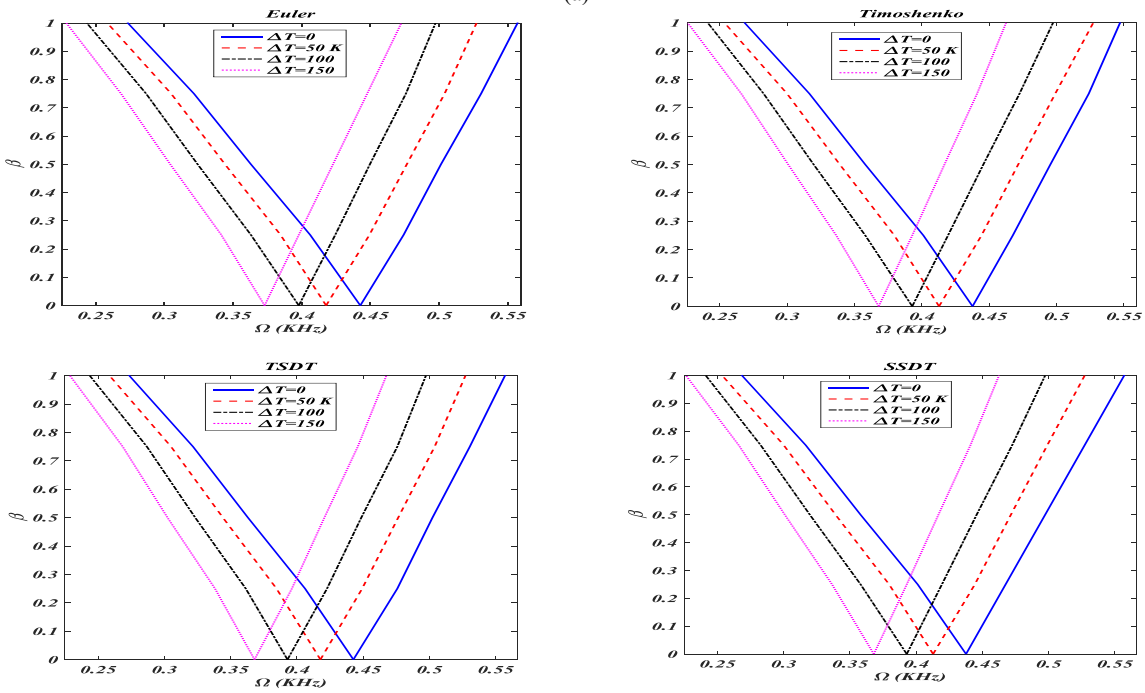

(b)

Fig.3
The dynamic stability regions of BDFGMs beam for different temperatures rise; a) power law model, b) exponential law model.

The influence of static load factor on the dynamic stability of BDFGMs beam is depicted in Fig. 4. As can be seen, increasing α leads to decrease the pulsation frequency and increase the dynamic instability region. This is expected as the increase of static load factor means the increase of the time independent component of the axial force which reduces the effective stiffness of the beam.

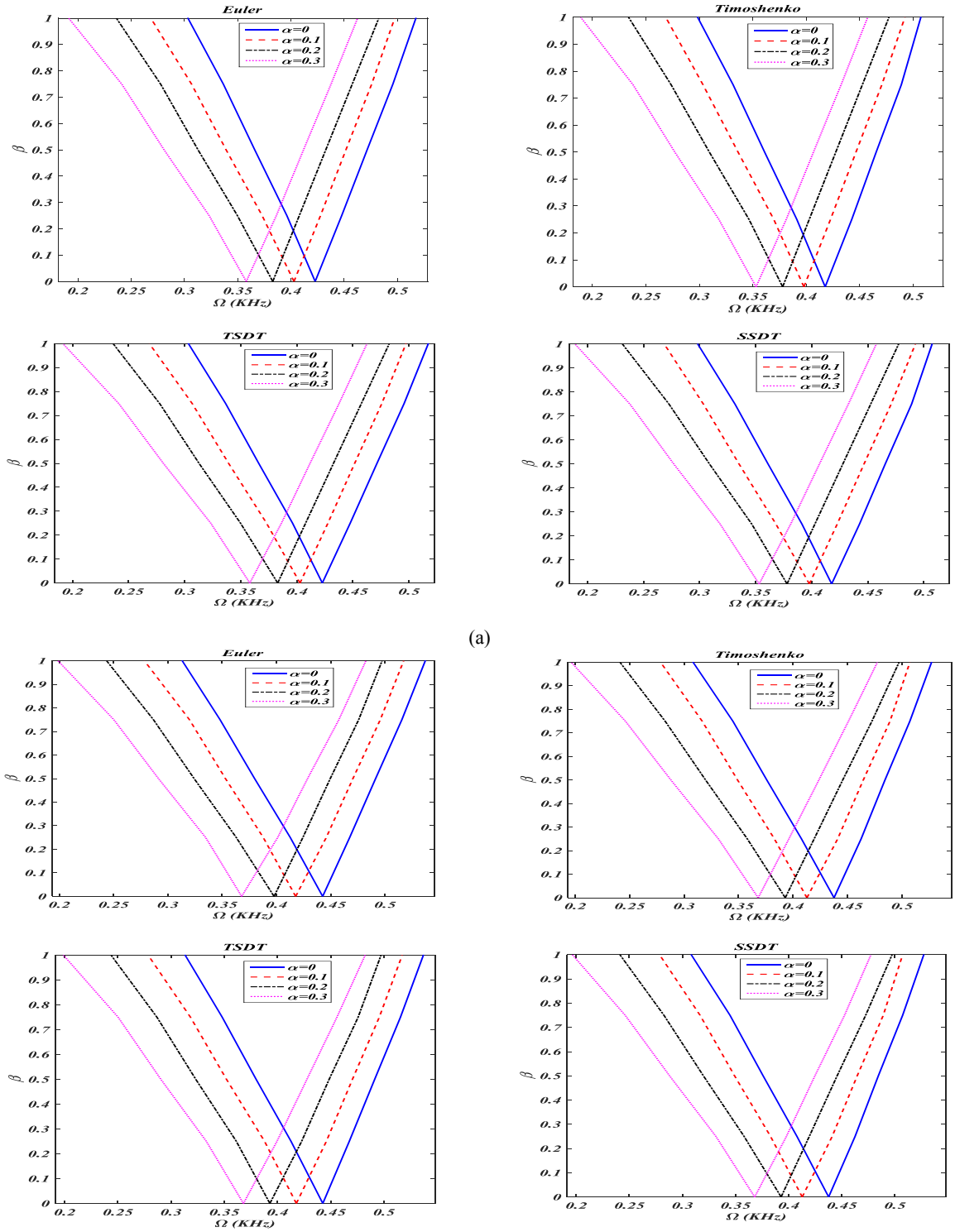

(a)

(b)

Fig.4
The dynamic stability regions of BDFGMs beam for different static load factor; a) power law model, b) exponential law model.

Figs. 5 and 6 show the dynamic stability regions of BDFGMs beam for different gradient indexes through in x and z directions, respectively. According to Fig. 5, increasing n_x leads to increase the pulsation frequency for both

power and exponential law models and will be approximately constant for $n_x \geq 3$. But from Fig. 6, it is evident that the instability region decreases by increasing n_z and shifts to the lower pulsation frequency. In addition, the effect of n_z is greater than n_x on the dynamic stability of BDFGMs beam by comparing the results obtained from Figs. 5 and 6.

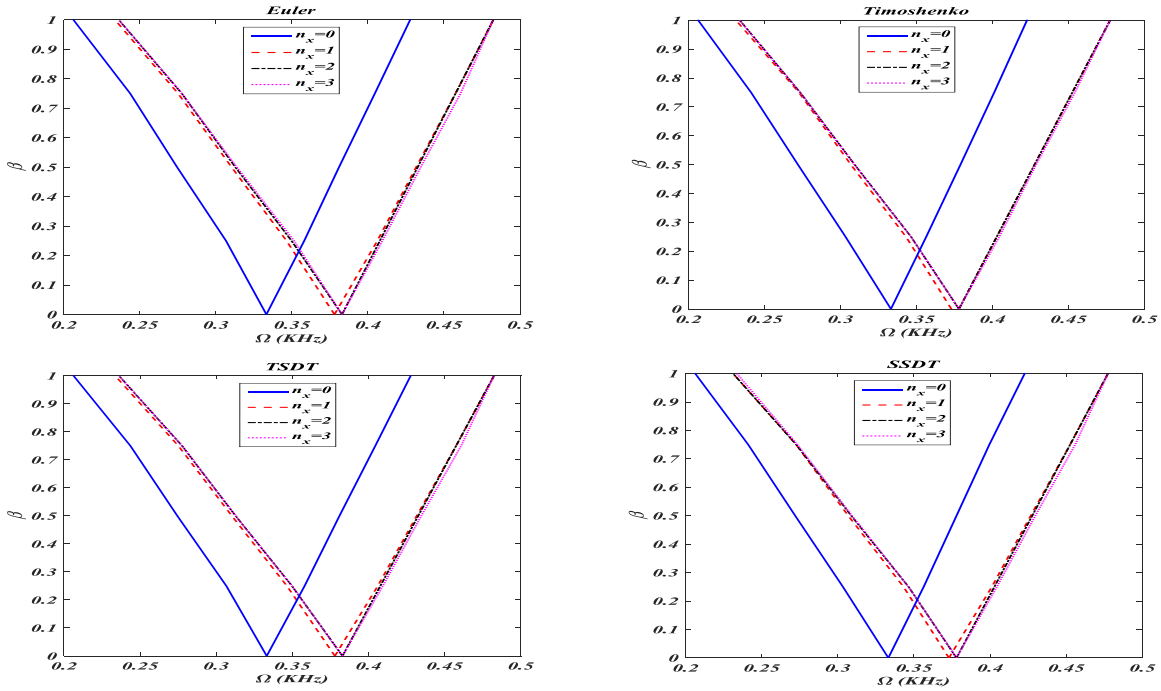

(a)

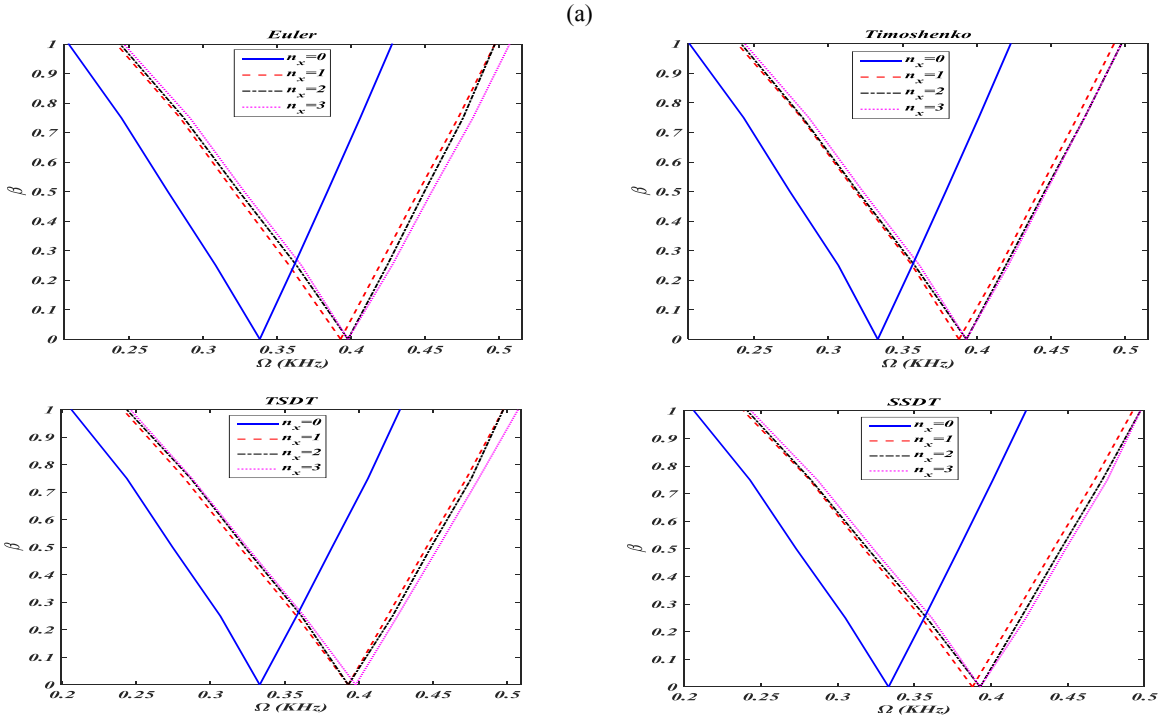

(b)

Fig.5
The dynamic stability regions of BDFGMs beam for different gradient index through in x direction (n_x); a) power law model, b) exponential law model.

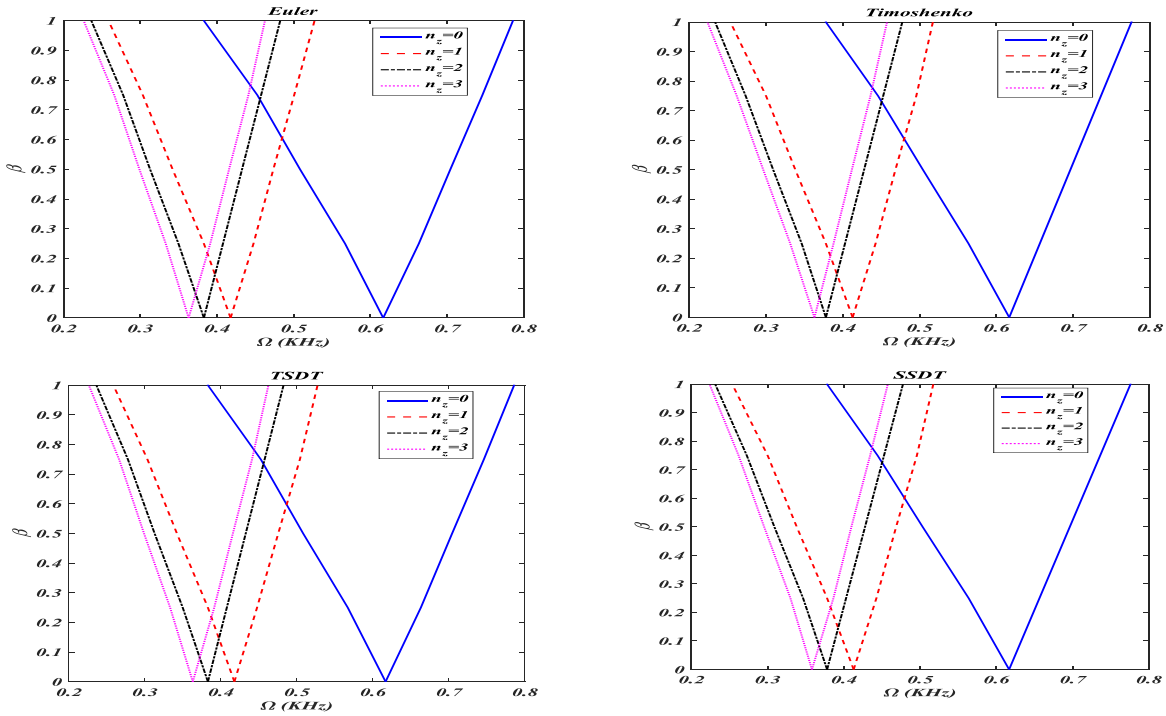

(a)

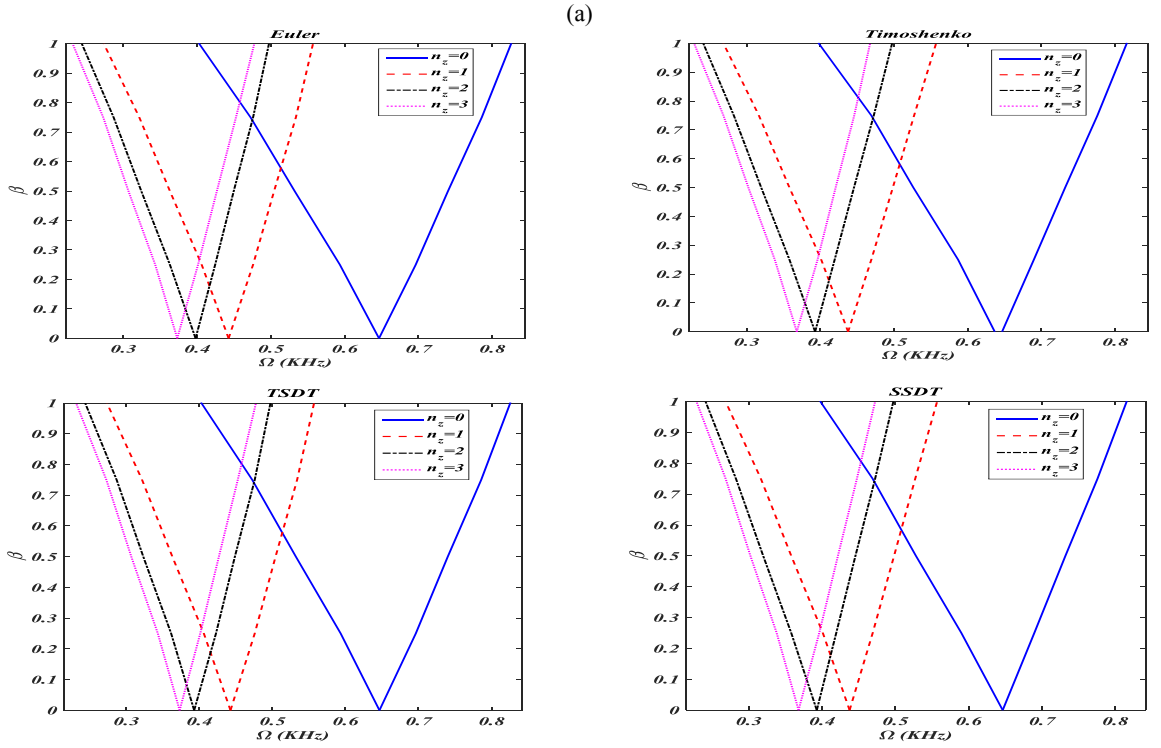

(b)

Fig.6
The dynamic stability regions of BDFGMs beam for different gradient index through in *z* direction (n_z); a) power law model, b) exponential law model.

The effect of thickness-to-length ratio on the dynamic stability regions of BDFGMs beam is demonstrated in Fig. 7. It can be concluded that the system becomes more stable and stiffer by increasing thickness-to-length ratio and therefore, the pulsation frequency increases and shifts to the right side of figure.

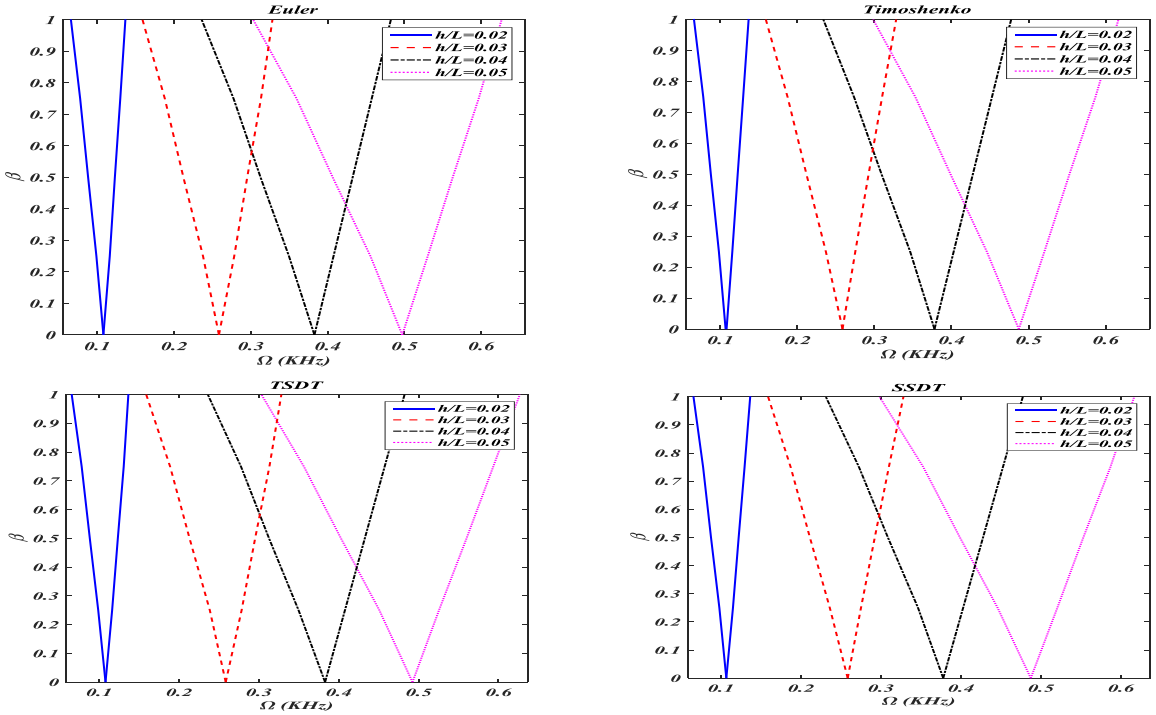

(a)

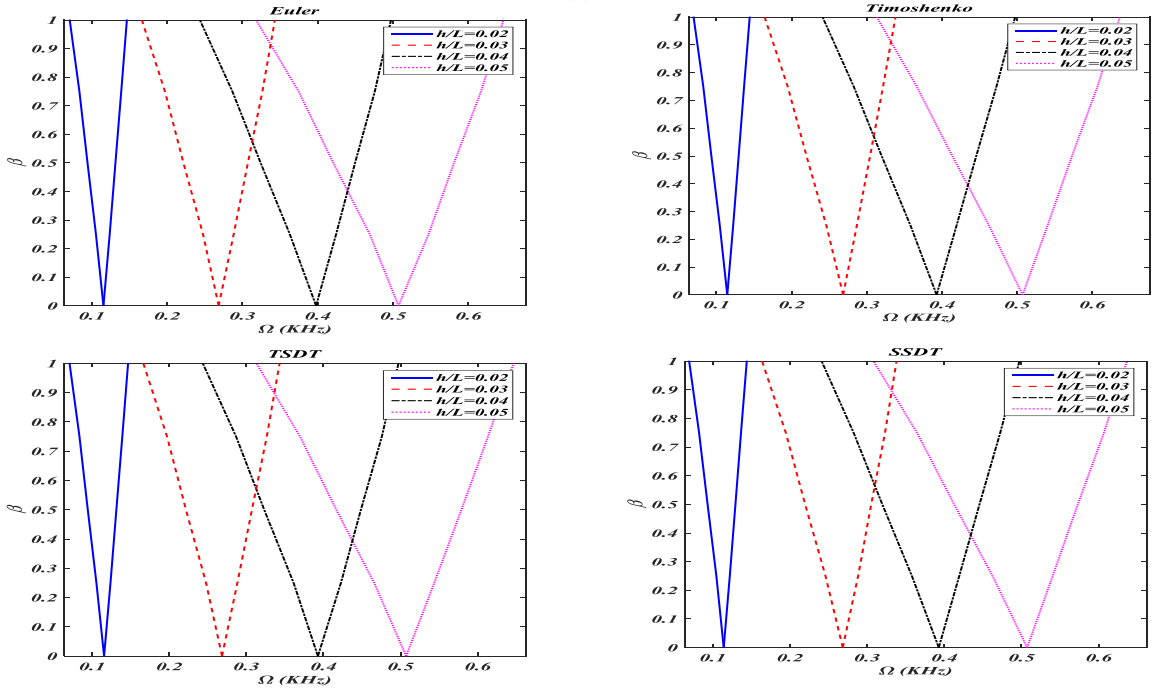

(b)

Fig.7
The dynamic stability regions of BDFGMs beam for different thickness-to-length ratios; a) power law model, b) exponential law model.

Fig. 8 presents the dynamic stability regions of BDFGMs beam for various foundation models. In order to study this issue, Four cases of foundation models are assumed as, case 1 (without foundation: ($K_w = 0, K_G = 0, C_d = 0$), case 2 (Winkler foundation: $K_w = 50 MN/m^3, K_G = 0, C_d = 0$), case 3 (Pasternak foundation: $K_w = 50 MN/m^3$,

$K_G = 10MN/m, C_d = 0$) and case 4 (visco-Pasternak foundation: $K_w = 50MN/m^3, K_G = 10MN/m, C_d = 10KNs/m^3$). It is obvious that the pulsation frequency increases by putting the system on the elastic foundation and the dynamic instability region moves to the larger pulsation frequency. Also, due to consider the influences of normal stresses and the transverse shear deformation by Pasternak model, it can be found that the dynamic instability region of case 3 is higher than that of Winkler or visco-Pasternak one.

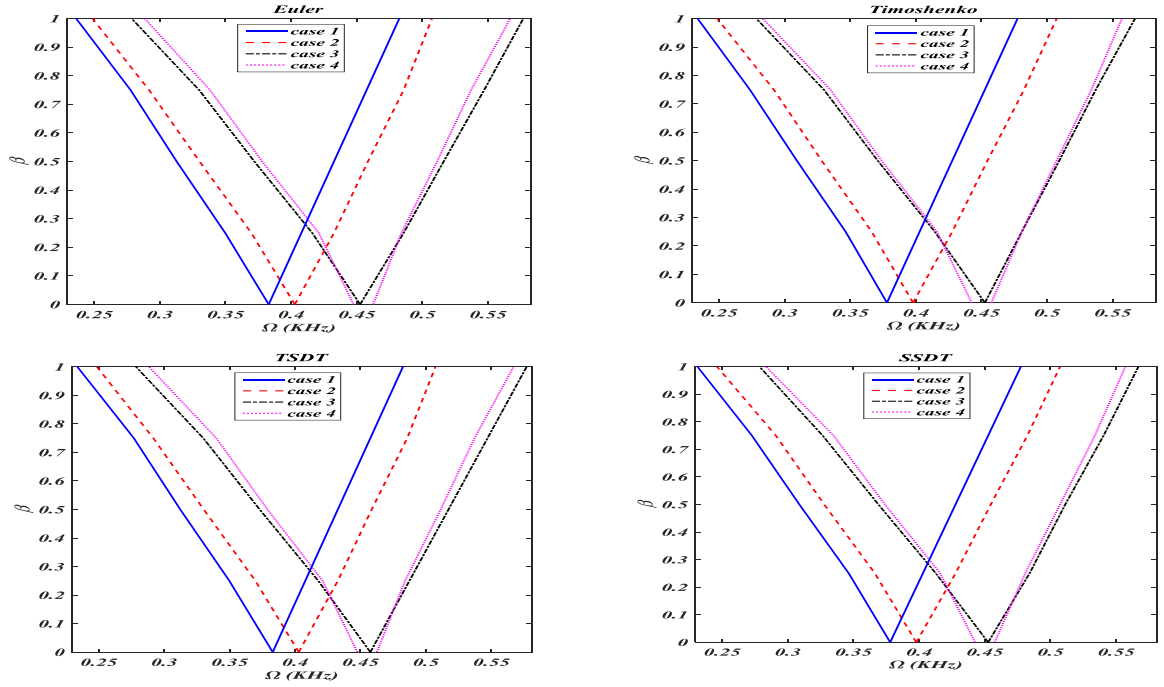

(a)

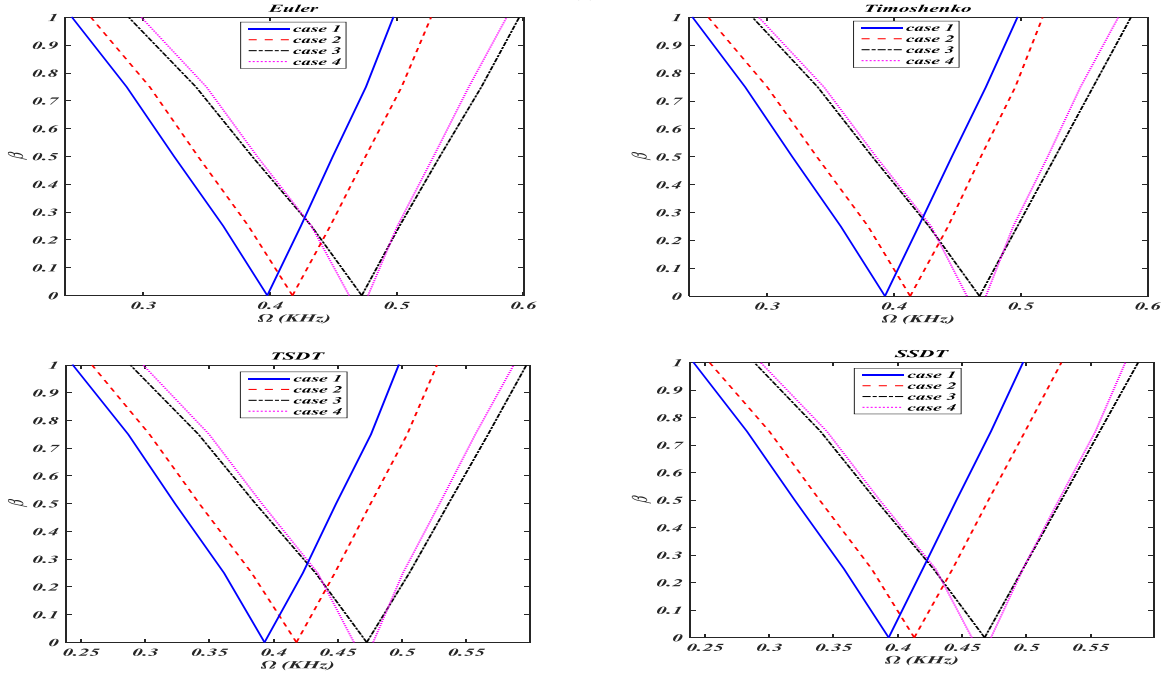

(b)

Fig.8
The dynamic stability regions of BDFGMs beam for various foundation models; a) power law model, b) exponential law model.

6 CONCLUSIONS

This research investigated the dynamic stability analysis of BDFGMs beam rested on visco-Pasternak foundation subjected to the harmonic excitation and thermal environment. By assuming temperature-dependent material properties, mechanical and thermal properties of beam obtained along the thickness and longitudinal directions according to the exponential and power law models. Based on EBT, TBT, TSDT and SSDT, the stability equations of BDFGMs beam derived using the Hamilton's principle and solved by GDQM in conjunction with the Bolotin method under SS, SC and CC boundary conditions. Then, the results of present work compared with the results found in the literature and a good agreement observed. The remarkable results are listed as follows:

- The pulsation frequency obtained by EBT is higher than that for other shear deformation beam theories and the results obtained by TBT, TSDT and SSDT are very close to each other.
- Considering exponential law model in order to determine the material properties of BDFGMs beam causes to obtain the larger pulsation frequency in comparison with power law model.
- The effect of gradient index of material properties along the thickness direction is greater than gradient index along the longitudinal direction on the dynamic stability of BDFGMs beam.
- The flexibility of BDFGMs beam increases under rising temperature and thus, the dynamic instability region shift to the lower pulsation frequency and decreases.

REFERENCES

[1] Li X.F., 2008, A unified approach for analyzing static and dynamic behaviors of functionally graded Timoshenko and Euler–Bernoulli beams, *Journal of Sound and Vibration* **318**(4-5): 1210-1229.

[2] Piovan M.T., Machado S.P., 2011, Thermoelastic dynamic stability of thin-walled beams with graded material properties, *Thin-Walled Structures* **49**(3): 437-447.

[3] Mohanty S.C., Dash R.R., Rout T., 2011, Parametric instability of a functionally graded Timoshenko beam on Winkler's elastic foundation, *Nuclear Engineering and Design* **241**(8): 2698-2715.

[4] Yan T., Kitipornchai S., Yang J., He X.Q., 2011, Dynamic behaviour of edge-cracked shear deformable functionally graded beams on an elastic foundation under a moving load, *Composite Structures* **93**(11): 2992-3001.

[5] Ke L.L., Wang Y.S., 2011, Size effect on dynamic stability of functionally graded microbeams based on a modified couple stress theory, *Composite Structures* **93**(2): 342-350.

[6] Şimşek M., Kocatürk T., Akbaş Ş.D., 2012, Dynamic behavior of an axially functionally graded beam under action of a moving harmonic load, *Composite Structures* **94**(8): 2358-2364.

[7] Salamat-talab M., Nateghi A., Torabi J., 2012, Static and dynamic analysis of third-order shear deformation FG micro beam based on modified couple stress theory, *International Journal of Mechanical Sciences* **57**(1): 63-73.

[8] Yan T., Yang J., Kitipornchai S., 2012, Nonlinear dynamic response of an edge-cracked functionally graded Timoshenko beam under parametric excitation, *Nonlinear Dynamics* **67**(1): 527-540.

[9] Yas M.H., Heshmati M., 2012, Dynamic analysis of functionally graded nanocomposite beams reinforced by randomly oriented carbon nanotube under the action of moving load, *Applied Mathematical Modelling* **36**(4): 1371-1394.

[10] Zamanzadeh M., Rezazadeh G., Jafarsadeghi-poornaki I., Shabani R., 2013, Static and dynamic stability modeling of a capacitive FGM micro-beam in presence of temperature changes, *Applied Mathematical Modelling* **37**(10-11): 6964-6978.

[11] Nguyen D.K., Gan B.S., Le T.H., 2013, Dynamic response of non-uniform functionally graded beams subjected to a variable speed moving load, *Journal of Computational Science and Technology* **7**(1): 12-27.

[12] Wattanasakulpong N., Mao Q., 2015, Dynamic response of Timoshenko functionally graded beams with classical and non-classical boundary conditions using Chebyshev collocation method, *Composite Structures* **119**: 346-354.

[13] Ghiasian S.E., Kiani Y., Eslami M.R., 2015, Nonlinear thermal dynamic buckling of FGM beams, *European Journal of Mechanics - A/Solids* **54**: 232-242.

[14] Gan B.S., Trinh T.H., Le T.H., Nguyen D.K., 2015, Dynamic response of non-uniform Timoshenko beams made of axially FGM subjected to multiple moving point loads, *Structural Engineering and Mechanics* **53**(5): 981-995.

[15] Wang Y., Wu D., 2016, Thermal effect on the dynamic response of axially functionally graded beam subjected to a moving harmonic load, *Acta Astronautica* **127**: 171-181.

[16] Malekzadeh P., Monajjemzadeh S.M., 2016, Dynamic response of functionally graded beams in a thermal environment under a moving load, *Mechanics of Advanced Materials and Structures* **23**(3): 248-258.

[17] Wu H., Yang J., Kitipornchai S., 2017, Dynamic instability of functionally graded multilayer graphene nanocomposite beams in thermal environment, *Composite Structures* **162**: 244-254.

[18] Saffari S., Hashemian M., Toghraie D., 2017, Dynamic stability of functionally graded nanobeam based on nonlocal Timoshenko theory considering surface effects, *Physica B: Condensed Matter* **520**: 97-105.

[19] Nguyen D.K., Bui V.T., 2017, Dynamic analysis of functionally graded Timoshenko beams in thermal environment using a higher-order hierarchical beam element, *Mathematical Problems in Engineering* **2017**: 7025750.
[20] Touloukian Y.S., 1967, *Thermophysical Properties of High Temperature Solid Materials*, New York, MacMillan.
[21] Karamanli A., 2017, Elastostatic analysis of two-directional functionally graded beams using various beam theories and Symmetric Smoothed Particle Hydrodynamics method, *Composite Structures* **160**: 653-669.
[22] Hao D., Wei C., 2016, Dynamic characteristics analysis of bi-directional functionally graded Timoshenko beams, *Composite Structures* **141**: 253-263.
[23] Ghorbanpour Arani A., Atabakhshian V., Loghman A., Shajari A.R., Amir S., 2012, Nonlinear vibration of embedded SWBNNTs based on nonlocal Timoshenko beam theory using DQ method, *Physica B: Condensed Matter* **407**(13): 2549-2555.
[24] Mohammadimehr M., Rousta Navi B., Ghorbanpour Arani A., 2017, Dynamic stability of modified strain gradient theory sinusoidal viscoelastic piezoelectric polymeric functionally graded single-walled carbon nanotubes reinforced nanocomposite plate considering surface stress and agglomeration effects under hydro-thermo-electro-magneto-mechanical loadings, *Mechanics of Advanced Materials and Structures* **24**(16):1325-1342.
[25] Ebrahimi F., Barati M.R., Haghi P., 2017, Thermal effects on wave propagation characteristics of rotating strain gradient temperature-dependent functionally graded nanoscale beams, *Journal of Thermal Stresses* **40**(5): 535-547.
[26] Ghorbanpour Arani A., Haghparast E., BabaAkbar Zarei H., 2016, Nonlocal vibration of axially moving graphene sheet resting on orthotropic visco-Pasternak foundation under longitudinal magnetic field, *Physica B: Condensed Matter* **495**: 35-49.
[27] Bellman R.E., Casti J., 1971, Differential quadrature and long term integration, *Journal of Mathematical Analysis and Applications* **34**: 235-238.
[28] Bolotin V.V., 1964, *The Dynamic Stability of Elastic Systems*, Holden-Day, San Francisco, CA.
[29] Ebrahimi F., Ghasemi F., Salari E., 2016, Investigating thermal effects on vibration behavior of temperature-dependent compositionally graded Euler beams with porosities, *Meccanica* **51**(1): 223-249.
[30] Thom T.T., Kien N.D., 2018, Free vibration analysis of 2-D FGM beams in thermal environment based on a new third-order shear deformation theory, *Vietnam Journal of Mechanics* **40**(2): 121-140.
[31] Nguyen D.K., Nguyen Q.H., Tran T.T., Bui V.T., 2017, Vibration of bi-dimensional functionally graded Timoshenko beams excited by a moving load, *Acta Mechanica* **228**(1): 141-155.